SUPPLEMENTAL FIGURES

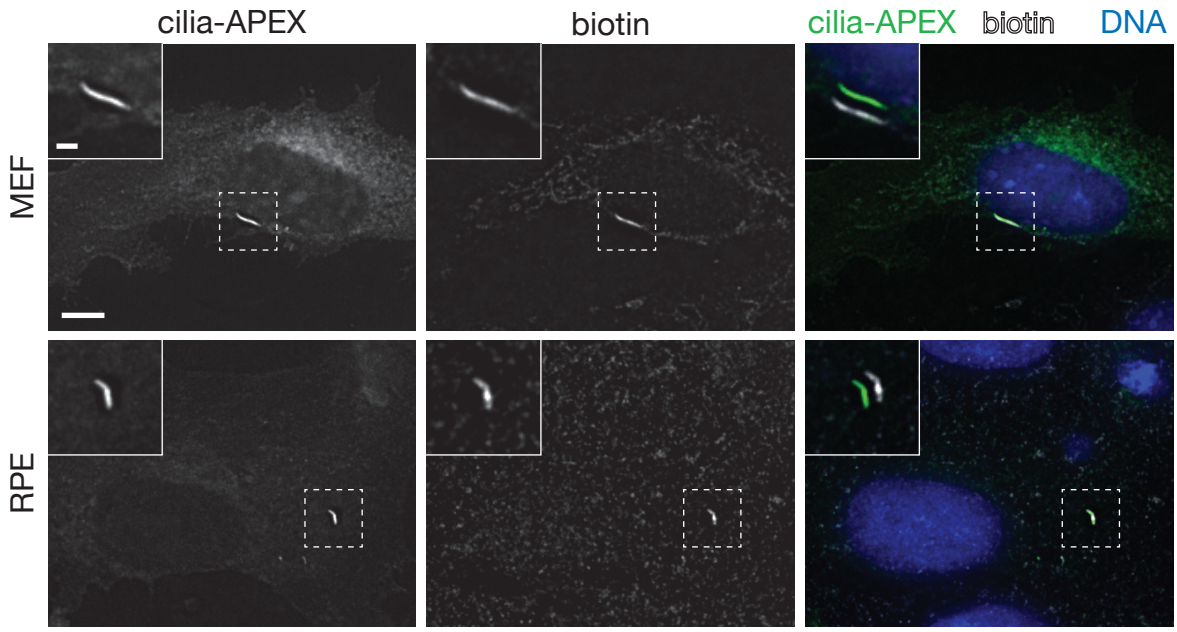

Figure S1 (related to Figure 1). Cilia-APEX achieves cilia-specific biotinylation in several cell types

Immunofluorescence of mouse embryonic fibroblast (MEF) and human retinal pigmented epithelial (RPE) cells after transient transfection with cilia-APEX. Cilia-APEX is detected by GFP fluorescence, biotinylated proteins by SA647. Merged insets show primary cilia with channels shifted to aid visualization. Scale bars are 5 μm (main panels) and 1 μm (insets). Note that merged images are also shown in Figure 1C.

A

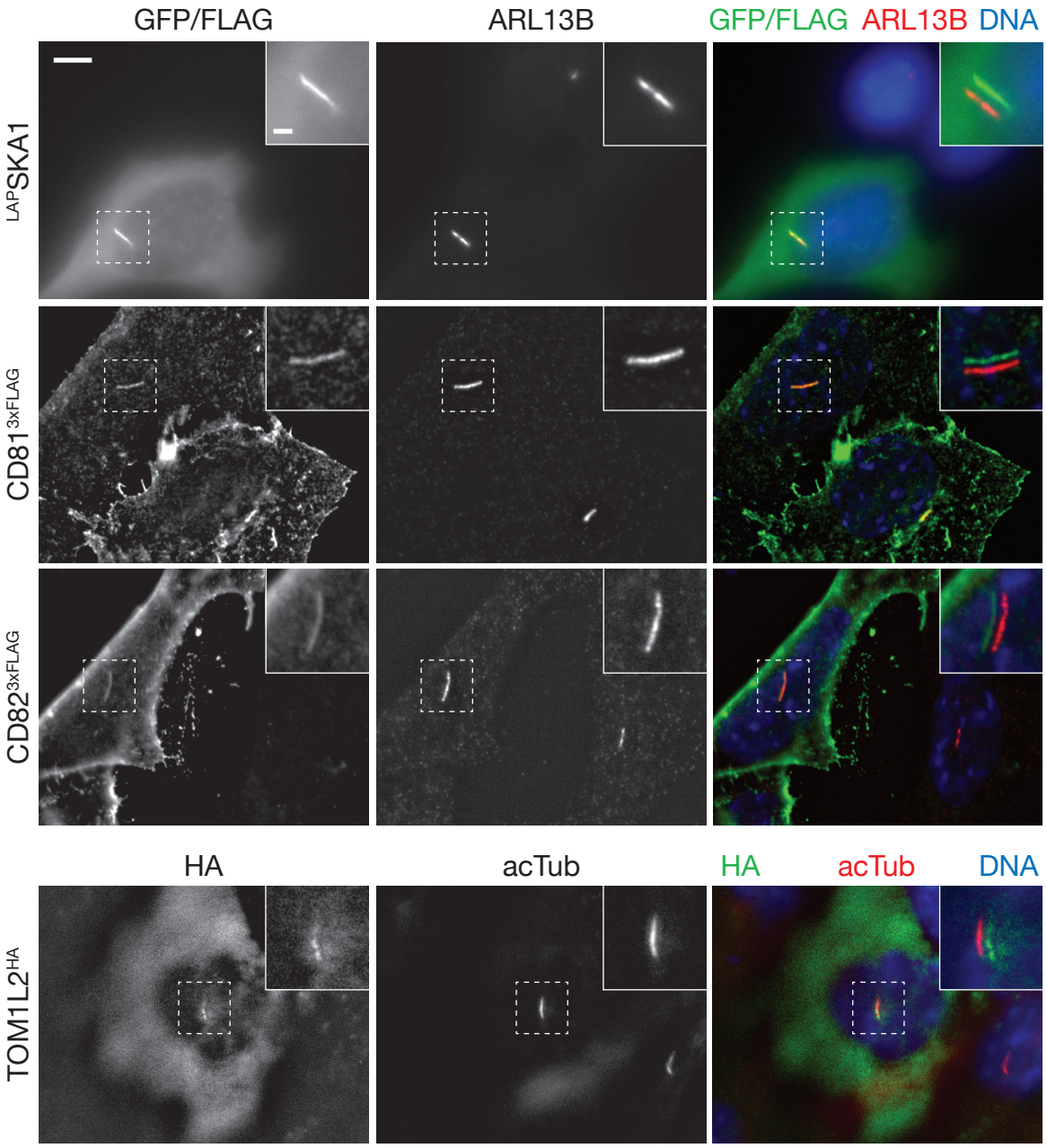

B

confirmed	not confirmed
ADCY6	CSNK 1E
AMPKβ2	GALECTIN3
CD81	ISLR
CD82	PBK
LKB1	TOM1
PKA RIα	VWA5A
SKA1	p97/VCP
STRADβ	
TOM1L2	

Figure S2 (related to Figure 2). Validation of candidate ciliary protein localization
See next page for legend.

Figure S2 (related to Figure 2). Validation of candidate ciliary protein localization

(A) IMCD3 cells were transiently transfected for 24 h, serum starved for another 24 h, fixed in 4% paraformaldehyde, and permeabilized with 0.1% Triton-X100. Proteins were detected by GFP fluorescence (LAP-SKA1), or immunofluorescence with anti-FLAG or anti-HA antibodies. Cilia were counterstained using anti-ARL13B or anti-acetylated tubulin antibodies as indicated. Merged insets show primary cilia with channels shifted to aid visualization. Scale bars represent 5 μm (main panels) and 1 μm (insets). Merged panels are also shown in Figure 2D.

(B) Table of candidate ciliary proteins, the localization of which were analyzed by immunofluorescence microscopy.

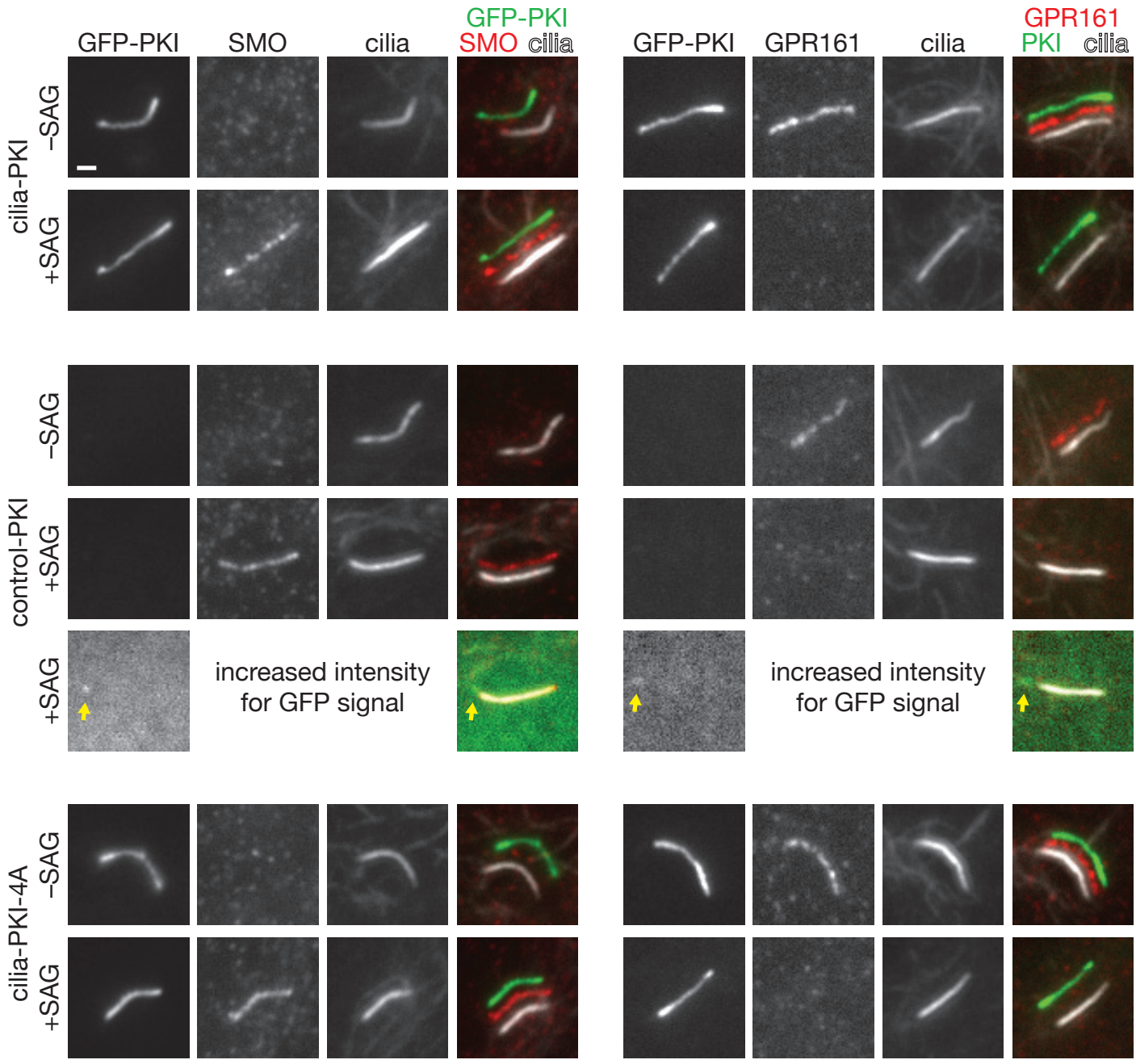

Figure S3 (related to Figure 4). Cells expressing cilia-PKI show normal redistribution of SMO to cilia and of GPR161 out of cilia upon Hh signal activation

Fluorescence microscopy of IMCD3 cells stably expressing the protein kinase A inhibitor peptide PKI, directed to cilia (cilia-PKI), to the cytoplasm (control-PKI) or a non-inhibiting mutant PKI-4A directed to cilia (cilia-PKI-4A) in the presence or absence of SAG. Anti-SMO, anti-GPR161 and anti-acetylated tubulin antibodies were used for immunofluorescence and PKI-constructs detected by GFP fluorescence. Higher intensity images are provided for control-PKI cells showing increased signal at the basal bodies (yellow arrows). Channels were shifted to aid visualization in merged images, except for higher intensity images showing GFP. Scale bar represents 1 μm. Merged panels of cilia-PKI cells are also shown in Figure 4C.

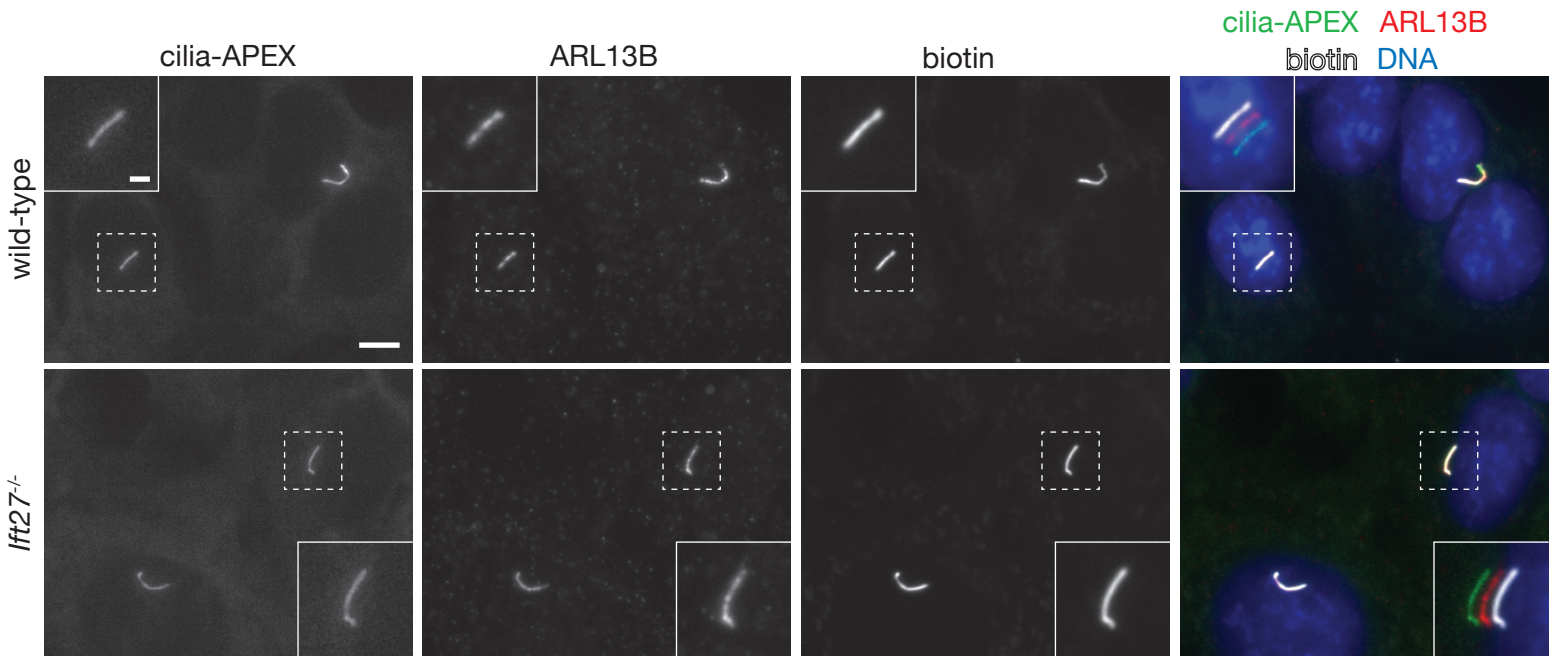

Figure S4 (related to Figure 6). APEX-mediated labeling in Ift27-/- and wild-type cells
Microscopic analysis of indicated cilia-APEX expressing cell lines after APEX-labeling by immunofluorescence was conducted as in Figure 1B. Cilia were counterstained using anti-ARL13B antibody; cilia-APEX is detected by GFP fluorescence, and biotinylated proteins by SA647. Scale bars are 5 μm (main panels) and 1 μm (insets).

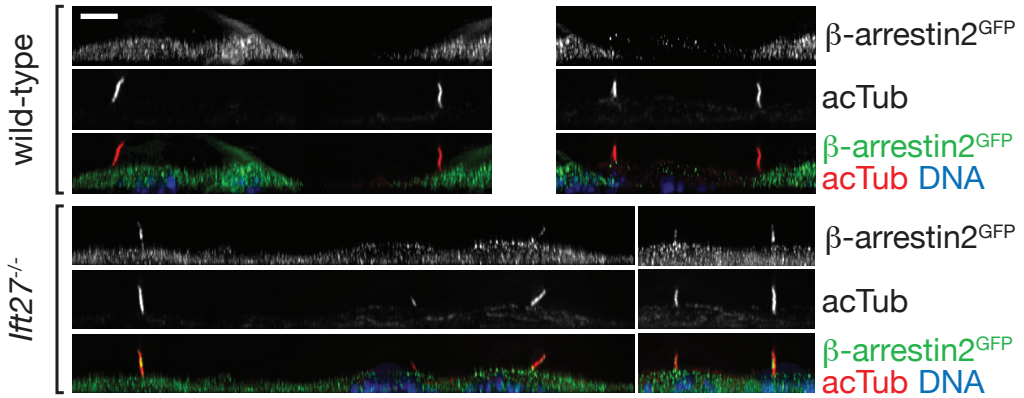

Figure S5 (related to Figure 7). XZ Projections of β-arrestin2-GFP expressing cells
Wild-type and Ift27-/- cells stably expressing β-arrestin2-GFP were analyzed by immunofluorescence as in Figure 7F. 45 planes from z-stacks acquired at 0.2 μm interval were deconvolved and used for 3D reconstruction. Images show XZ projections to visualize apical cilia. Scale bar represents 5 μm.

SUPPLEMENTAL TABLES

Table S1 (related to Figure 2). Candidate ciliary proteins identified by cilia-APEX

List of proteins specifically identified by cilia-APEX in three independent experiments. Total spectral counts as well as the number of experimental repeats in which proteins were identified are indicated. Note that hits are displayed in two sheets, corresponding to Tier1 and Tier2 hits (see main text for details).

Table S2 (related to Figure 6). Quantitative proteomics of wild-type versus *Ift27*$^{-/-}$ cilia

Proteins identified from wild-type and *Ift27*$^{-/-}$ cilia-APEX lines. Individual spectral counts (SpC) from three independent experiments as well as averages are shown. SpCs of 0 have been replaced by 0.25 for quantification purposes (see Supplementary Experimental Procedures for details). Proteins are shown in descending order of enrichment in *Ift27*$^{-/-}$ over wild-type. Black horizontal lines indicate significance thresholds (see main text for details).

SUPPLEMENTARY EXPERIMENTAL PROCEDURES

Plasmids and Antibodies

Most constructs were generated using the Gateway cloning system (Life technologies) and maps are available upon request. Soybean APEX (Rhee et al., 2013) was introduced into the FlpIn destination vector pEF5B-DEST/FRT by isothermal assembly to generate pEF5B-DEST-APEX/FRT for C-terminal tagging. NPHP3[1-203]-GFP was gene synthesized without a Stop codon and introduced into pDONR221 to generate pENTR-NPHP3[1-203]-GFP. A G2A mutation in NPHP3[1-203] was introduced by site-directed mutagenesis, and the respective entry vectors were recombined into pEF5B-DEST-APEX/FRT to generate pEF5B-NPHP3[1-203]-GFP-APEX/FRT (cilia-APEX) and pEF5B-NPHP3[1-203; G2A]-GFP-APEX/FRT (control-APEX). Cilia-PKI, cilia-PKI-4A and control-PKI were generated by primer-extension overlap PCR including respective PKI and PKI-4A sequences (Iglesias-Bartolome et al., 2015) in the oligonucleotides to fuse them to NPHP3[1-203]-GFP and the G2A mutant under the control of a truncated CMV promotor. NG-PKA-RIα and NG-AMPKβ2 were generated by LR clonase reaction of pEF5/FRT/NG-DEST with pENTR-PRKAR1A and pENTR-PRKAB2, respectively. LKB1-NG, STRADα-3xFLAG, STRADβ-3xFLAG, CD81-3xFLAG and CD82-3xFLAG were generated by recombination of the respective entry vectors without Stop codons into destination vectors. Genes of interest were cloned from IMCD3 cDNA (STRADβ, CD81, CD82), obtained from Addgene (APEX, PRKAR1A, PRKAB2, LKB1, STRADα) or generously provided by Iain Cheeseman (GFP-SKA1) and Mark Scott (GFP-β-arrestin2). C6S and C8S mutations were introduced into STRADβ by site-directed mutagenesis.

Antibodies against the following antigens were used: acetylated tubulin (611B1, Sigma), glutamylated tubulin (GT335, gift from Carsten Janke), ARL13B (gift from Tamara Caspari), LKB1 (Cell Signaling), AC5/6 (Fabgennix), AC3 (Santa Cruz), CLUAP1 (gift from Hiroshi Hamada), CAR (gift from Jeff Bergelson), SMO (gift from Kathryn Anderson), GPR161 (gift from Saikat Mukhopadhyay), GLI3 (gift from Suzie Scales), Ninein (gift from Michel Bornens), CEP290 (gift from Sophie Saunier), GFP (Invitrogen), IFT88 (Proteintech), tubulin (DM1A), actin (Sigma), ANXA5 (Abcam) and GAPDH (Abcam). Biotinylated proteins were detected using streptavidin-polyHRP (Thermo Scientific) or streptavidin coupled to AlexaFluor647 (Ye et al., 2013).

Cell culture and generation of stable cell lines

IMCD3 and RPE1-hTERT cells were cultured in DMEM/F12 medium supplemented with 10% FBS (Gemini), 100 U/ml penicillin-G and 100 µg/ml streptomycin. MEFs were grown in DMEM with the same supplements. Ciliation was induced by starvation in media containing 0.2% FBS for 16-24 h, as indicated. Transfections were preformed using XtremeGene9 (Roche) or Lipofectamine 2000 (Life technologies), according to manufacturers guidelines. Stable IMCD3 cell lines expressing cilia-APEX, control-APEX, cilia-PKI, control-PKI, cilia-PKI-4A, NG-PKA-RIα and NG-AMPKβ2 were generated using the FlpIn system as described (Breslow and Nachury, 2015). *Ift27*$^{-/-}$ IMCD3 cells were generated by CRISPR/Cas9-mediated genome editing (Liew et al., 2014). Mouse neurons were isolated by decapitating P0 mice and dissecting the cortex. Single cells were obtained by papain digestion, trituration and straining. Cells were plated onto matrigel-treated coverslips and grown in Eagle's MEM supplemented with 1% glucose, 0.4% $NaHCO_3$, 0.2 mg/ml transferrin, 4 mM L-glutamine and 2 µM arabinofuranosyl cytidine.

Synthesis of biotin-phenol

Biotin-phenol was synthesized in a one step ligation of biotin and tyramine (Sigma) according to published procedures (Rhee et al., 2013). In brief, after stirring biotin with 1.1 equivalents of HATU (2-(7-aza-1H-benzotriazole-1-yl)-1,1,3,3-tetramethyluronium hexafluorophosphate) and 3.0 equivalents of Hünig's base (*N*,*N*-Diisopropylethylamine, Sigma) in dimethyl sulfoxide (DMSO) for 10 min at room temperature, equimolar amounts of tyramine were added and stirred overnight. Products were purified on a C18 reverse phase column by high-pressure liquid chromatography (HPLC). A 5 to 95% gradient of acetonitrile in H_2O was applied and fractions collected while monitoring UV-absorption. Fractions of interest were pooled and products vacuum-dried. Purity of the resulting compound was assessed by MALDI-TOF mass spectrometry and NMR.

Immunofluorescence Microscopy

Cells were grown on acid-washed 12 mm #1.5 coverslips and fixed in 4% paraformaldehyde for 15 min at 37°C or room temperature. After fixation cells were permeabilized in blocking buffer (3% bovine serum albumin, 5% normal donkey serum in 1x PBS) containing 0.1% Triton-X100

for 10 min or 0.1% saponin for 30 min. After permeabilization, cells were blocked in blocking buffer without detergent for additional 30 min. Subsequently, cells were incubated with primary antibodies diluted in blocking buffer for 1 hr at room temperature, washed five times with PBS over 15 minutes and incubated with AlexaFluor488-, AlexaFluor647- or Cy3-conjugated secondary antibodies (Jackson Immunoresearch), or AlexaFluor647-coupled streptavidin in blocking buffer. Lastly, cells were washed five times in PBS and stained with Hoechst DNA dye before mounting on slides using Fluoromount G (Electron Microscopy Sciences).

Cells were imaged on a DeltaVision system (Applied Precision) with a PlanApochromat oil objective (60x/1.4NA) or on an AxioImager.M1 microscope (Carl Zeiss) with a PlanApochromat oil objective (63x/1.4NA) using appropriate filters. Images were captured using a sCMOS (Applied Precision) or CoolSNAP HQ (Photometrics) camera system, respectively.

Mass spectrometric analyses

After FASP, the proteolytic peptides were captured in the flow-through of the filters and cleaned on C18 stage tips. Peptides were separated on a Nano-Acquity HPLC (Waters) run at 300 nL/min where mobile phase A was 0.585% acetic acid in Water and mobile phase B was 0.585% acetic acid, 90% acetonitrile, 9.415% water. Dried peptide pools were reconstituted in mobile phase A and injected onto a 20cm fused silica C18 reverse phase column that was packed in-house using 3 μM C18 particles (PEEKE Scientific). The mass spectrometer was a LTQ Orbitrap Velos operated in data dependent acquisition (DDA) mode to fragment the 15 most intense multiply charged precursor cations in a High-Low schema, where the resolution in the orbitrap was set to 60K and ion trap MSMS occurred with a precursor selection window of 1.8Da with a maximum fill time of 10 milliseconds.

MS/MS data were analyzed using both Preview and Byonic v1.4 (ProteinMetrics). All data were first analyzed in Preview to provide recalibration criteria and then reformatted to .MGF before full analysis with Byonic. Analyses used Uniprot canonical .fasta files for *Mus musculus*, concatenated with cilia-APEX and common contaminant proteins. Data were searched at 10 ppm mass tolerances for precursors, with 0.5 Da fragment mass tolerances assuming up to two missed cleavages and allowing for N-ragged tryptic digestion. These data were validated at a 2% false discovery rate (FDR) using typical reverse-decoy techniques (Elias and Gygi, 2007). The resulting identified peptide spectral matches and assigned proteins were then exported for

further analysis using custom tools developed in MatLab (MathWorks) to provide visualization and statistical characterization.

Comparative Mass spectrometric analyses

Ift27$^{-/-}$ and WT cilia proteins were purified using the cilia-APEX strategy in triplicate. Tryptic peptides were desalted by C18 SPE (Empore, 3M), eluted, and dried under vacuum. Peptides were resuspended in 5% formic acid and 5% acetonitrile and analyzed by LC/MS-MS on an Orbitrap Fusion mass spectrometer (Thermo Fisher Scientific) coupled to a Proxeon EASY-nLC II liquid chromatography (LC) pump (Thermo Fisher Scientific). Peptides were fractionated on a 75μm inner diameter microcapillary column packed with ~0.5 cm of Magic C4 resin (5μm, 100 Å, Michrom Bioresources) followed by ~35 cm of GP-18 resin (1.8 μm, 200 Å, Sepax). Approximately 1/10th of samples were loaded onto the column for analysis.

Peptides were separated using a 1 h gradient of 5 to 21% acetonitrile in 0.125% formic acid at a flow rate of ~500 nL/min. MS1 scans were detected in the Orbitrap with a resolution of 120,000, scan range of 400-1400 m/z, and maximum injection time of 100 ms. The most intense species from each MS1 was isolated in the quadrupole (isolation window 0.7) and fragmented by CID (collision energy 30%). MS2 spectra were detected in the Ion Trap using Ion Trap Rapid Scan Rate, a maximum injection time of 150 ms, and a normalized collision energy of 35.

Mass spectra were processed using an in-house software pipeline (Elias and Gygi, 2007). Spectra were converted to mzXML using a modified version of ReAdW.exe and searched against all entries from the mouse Uniprot database with the addition of common contaminants and the cilia-APEX fusion protein concatenated to a reverse sequence database using the SEQUEST algorithm using a 50 ppm precursor ion tolerance, trypsin protease specificity, and allowing for two missed cleavages. Peptides were filtered to a 1% false discovery rate (FDR) using linear discriminant analysis. Peptides were further assembled into proteins, which were further filtered to a 1% FDR. Redundant peptides were assigned to the protein with the most spectral evidence.

Raw spectral counts were used to calculate a normalized spectral abundance factor (NSAF) for each protein as previously described (Zybailov et al., 2006). Zero spectral counts were replaced by 0.25 determined empirically based on the distribution of log(NSAF) values. Mean spectral counts were calculated for each genotype and used to determine the *Ift27*$^{-/-}$ to WT

ratio for each protein. Proteins with mean spectral counts below 2.5 were excluded from analysis.

SUPPLEMENTARY REFERENCES

Breslow, D., and Nachury, M.V. (2015). Analysis of soluble protein entry into primary cilia using semipermeabilized cells. Methods Cell Biol 127, 203–221.

Elias, J.E., and Gygi, S.P. (2007). Target-decoy search strategy for increased confidence in large-scale protein identifications by mass spectrometry. Nat Methods 4, 207–214.

Iglesias-Bartolome, R., Torres, D., Marone, R., Feng, X., Martin, D., Simaan, M., Chen, M., Weinstein, L.S., Taylor, S.S., Molinolo, A.A., et al. (2015). Inactivation of a Gα(s)-PKA tumour suppressor pathway in skin stem cells initiates basal-cell carcinogenesis. Nat Cell Biol 17, 793–803.

Liew, G.M., Liew, G.M., Ye, F., Nager, A.R., Murphy, J.P., Lee, J.S., Aguiar, M., Breslow, D., Gygi, S.P., et al. (2014). The intraflagellar transport protein IFT27 promotes BBSome exit from cilia through the GTPase ARL6/BBS3. Dev Cell 31, 265–278.

Rhee, H.-W., Zou, P., Udeshi, N.D., Martell, J.D., Mootha, V.K., Carr, S.A., and Ting, A.Y. (2013). Proteomic mapping of mitochondria in living cells via spatially restricted enzymatic tagging. Science 339, 1328–1331.

Ye, F., Breslow, D., Koslover, E.F., Spakowitz, A.J., Nelson, W.J., and Nachury, M.V. (2013). Single molecule imaging reveals a major role for diffusion in the exploration of ciliary space by signaling receptors. Elife 2, e00654.

Zybailov, B., Mosley, A.L., Sardiu, M.E., Coleman, M.K., Florens, L., and Washburn, M.P. (2006). Statistical analysis of membrane proteome expression changes in Saccharomyces cerevisiae. J Proteome Res 5, 2339–2347.